

SWAP-C Ka-Band High Power Duplexer Based on the Emerging AFSIW Technology

15-18 October 2024

ESA/ESTEC, Noordwijk, The Netherlands

Issam Marah⁽¹⁾, Anthony Ghiotto⁽²⁾, Jean-Christophe Plumecoq⁽¹⁾, Savas Kurt⁽¹⁾ and Richard Tyan⁽¹⁾

⁽¹⁾*Exens-Solutions*

3 avenue du pacifique, 91940 Les Ulis, France
issam.marah@exens-solutions.com

⁽²⁾*Bordeaux Institute of Technology*

University of Bordeaux, IMS, CNRS UMR 5218, Bordeaux INP,
Talence, France
anthony.ghiotto@bordeaux-inp.fr

INTRODUCTION

The emergence of new space applications, particularly satellite constellations for telecommunications and surveillance services, poses significant challenges for satellite payloads. Over the past decade, the space industry has experienced a considerable shift towards "democratization," largely driven by the influx of new companies. Consequently, this has led to the introduction of new requirements for payloads, emphasizing mass production while simultaneously optimizing Size, Weight, Power, and Cost (SWAP-C), without compromising reliability and performance.

Among the components of satellite payloads microwave multiplexers are essential for separating or combining different frequency bands in satellite communications [1]. Various configurations of input multiplexers (IMUX) [1]-[3] are employed, particularly in multi-beam payloads. In such systems, signals received by the IMUX, after undergoing different frequency conversions, are routed to high-power amplifiers (HPAs). The architecture often requires many wideband multiplexers, making SWAP-C critical design factors for these components.

In this paper, the design of an Air-Filled Substrate Integrated Waveguide (AFSIW) duplexer interconnected with waveguides operating in the Ka-band for downlink communication is presented. The design adheres to industrial specifications while aiming for SWAP-C savings. The design revolves around two coupled channel filters via a double-junction composed of a circulator and an isolator.

Firstly, for duplexer interconnection, exploration of a waveguide to AFSIW transition is conducted. The transition is designed based on impedance transformers implemented by steps integrated into the waveguide and multilayer Printed Circuit Board (PCB) of the AFSIW line. Realization and measurement of the waveguide to AFSIW transition demonstrate low insertion loss and a wide bandwidth operation. The design is enhanced by integrating tuning screws to compensate for manufacturing tolerances and improve production yield.

Subsequently, the core element of the duplexer, comprising a double-junction (circulator and isolator), is designed by integrating a wideband circulator and a load. Mild steel brackets are employed to optimize the dual-junction's polarization and ensure its magnetostatic seal. For demonstration purposes, the isolator is fabricated and tested under weak signal conditions.

Once all the elementary building blocks of the duplexer were completed and validated, the channel filters were synthesized and integrated with the other components of the duplexer. The AFSIW duplexer was then fabricated, assembled, and measured under low signal conditions.

DUPLEXER BUILDING BLOCS DESCRIPTION

The configuration illustrated in Figure 1 employs isolated bandpass filters with dual junctions that include circulators and isolators. This design ensures that each channel filter operates independently, without interference from others. It is particularly advantageous in space applications due to its robustness: variations in one channel's impedance do not impact the others. The circulators provide effective isolation between filters, facilitating their independent design.

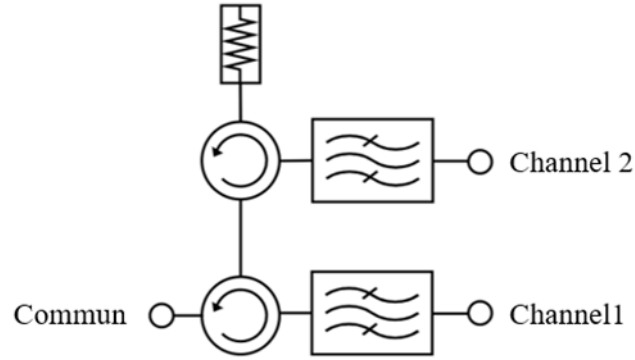


Figure 1. Duplexer synoptic.

Waveguide to AFSIW Interconnexion

For the interconnection of AFSIW equipment, several transitions have been proposed in the literature, focusing on coplanar or microstrip lines. However, the use of coplanar lines to excite the duplexer is limited by two factors: the insertion losses, which increase the noise figure for duplexer operation in reception mode, and the power handling capability of the coplanar line.

The waveguide to AFSIW transition will provide the advantages of high-power handling for RF transmission applications and low insertion losses for RF reception applications. The first horizontal waveguide transition to AFSIW was presented in 2017 [4]. It is based on the same principle as the waveguide transition to AFSIW presented in [5]. This transition is illustrated in Figure 2. It is designed with a progressive impedance matching modeled by sections of waveguide of different heights. Such a waveguide to AFSIW transition allows for impedance matching over a wide bandwidth of 30% in the Ka band, with low insertion and return loss (less than 0.1 dB and 25 dB, respectively). Tested under vacuum, the power handling capability of this transition exceeds 200 W. However, the horizontal aspect of this transition limits its use in AFSIW technology embedded systems. It has only been used for measurements to electrically characterize AFSIW circuits in both high and low signal conditions.

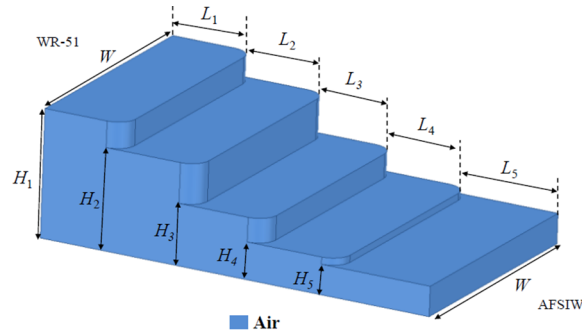


Figure 2. Waveguide to AFSIW horizontal transition [4] and [5].

For the interconnection of the duplexer, a new vertical waveguide transition to AFSIW is proposed (see Figure 3). It consists of two identical WR51 flanges, coupled with the AFSIW line through an opening in the substrate S1. Substrates S1 and S2 are used for impedance matching between the vertical waveguide and the horizontal AFSIW line. The impedance matching in such a transition involves matching the electric field lines of the horizontal TE₁₀ modes of the waveguide.

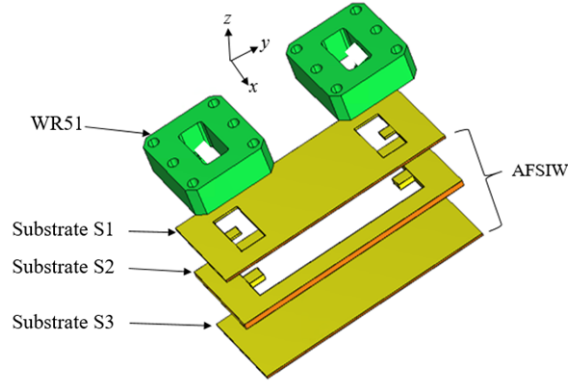
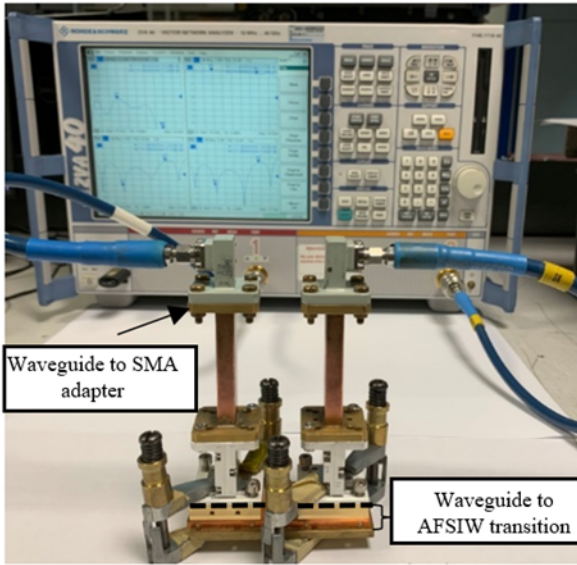
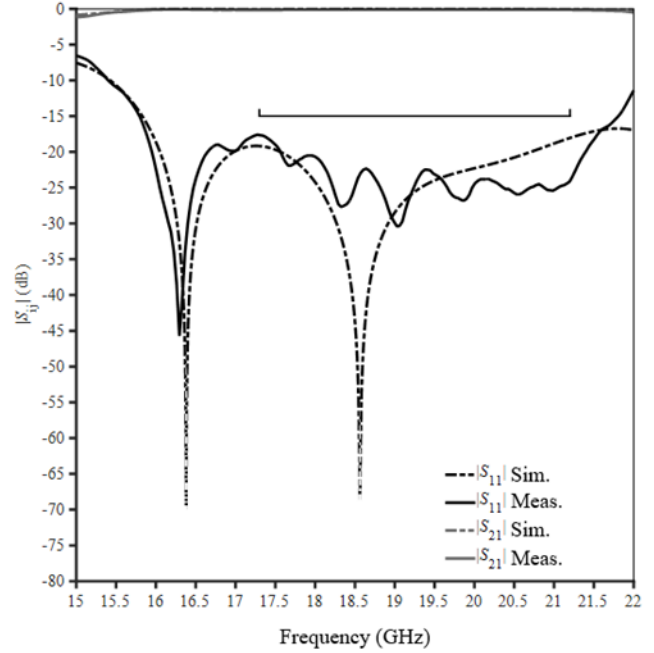


Figure 3. Waveguide to AFSIW vertical transition

The proposed waveguide to AFSIW transition was fabricated using three layers of RT/Duroid 6002 substrate. Substrate S2 has a thickness of $H = 1.524$ mm, identical to the thickness chosen in the previous section. The thicknesses of substrates S1 (H_{s1}) and S3 (H_{s3}) are $H_{s1} = H_{s3} = 0.508$ mm. A standard Thru, reflect and line (TRL) waveguide WR51 calibration kit was used to eliminate the effects of cables and transitions from waveguide to coaxial, allowing for the measurement of the transition in its plane. Figure 4(a) illustrates a photo of the waveguide to AFSIW transition during low signal measurements. The results of simulations and measurements are shown in Figure 4(b) and demonstrate the performance of the waveguide to AFSIW transition, with insertion losses of less than 0.2 dB and return losses greater than 18 dB in the frequency range from 16 GHz to 21.5 GHz.



(a)



(b)

Figure 4. (a) DUT and (b) Waveguide to AFSIW transition S-parameter.

Isolator Design

The isolator used in the design of the duplexer consists of a circulator junction with one path coupled to channel 2 of the duplexer and another path terminated with a matched load. To ensure independent operation of both channels, the isolator must accommodate the two frequency bands of operation of the duplexer. Therefore, a broadband design of the isolator is required.

In this section, the design of a Y-junction AFSIW circulator is presented, incorporating two asymmetrical gyromagnetic posts [6]. The proposed topology is illustrated in Figure 5(b). It features two ferrite disks, denoted as ferrite 1 and ferrite 2, positioned at the bottom and top center of the waveguide Y-junction, respectively, and separated by air (or vacuum in space). The ferrites differ in diameter, with D_{f1} and D_{f2} , and height, with H_{f1} and H_{f2} . The larger ferrite disk at the bottom is responsible for establishing the circulation conditions, while the smaller ferrite disk at the top improve the impedance matching between the ferrite loaded junction and three waveguide arms.

The patented circulator topology from Exens-Solutions [7] is a pioneering design, utilizing ferrite not only for its non-reciprocal properties but also for impedance matching. This approach enhances the utility of ferrite, reducing the reliance on conventional ridge transformers typically used in commercial circulators shown in Figure 5(a). Consequently, this topology presents a strong candidate for AFSIW technology, eliminating the need for ridges, which are costly to fabricate with PCB.

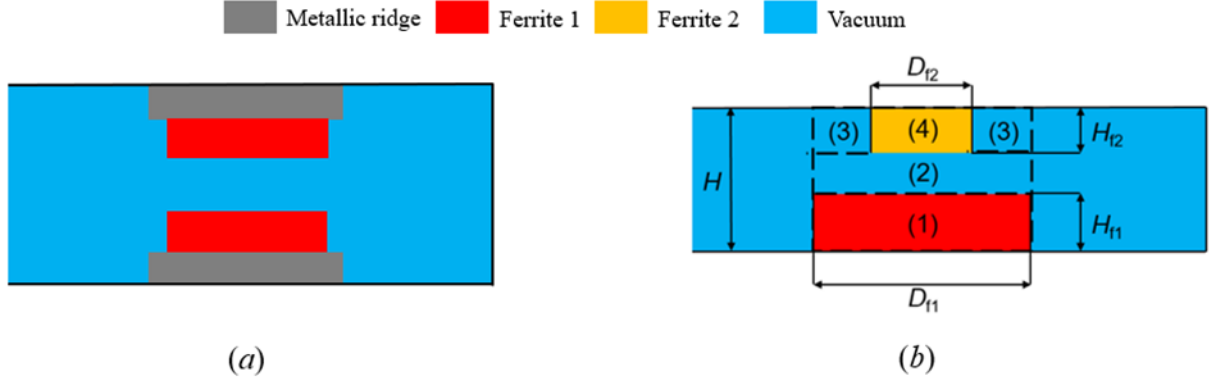


Figure 5. (a) commercial conventional circulator junction and (b): proposed circulator junction without metallic ridge.

The ferrite 1 disk achieves the circulation. It acts as a magnetized planar resonator involving a pair of rotational hybrid modes: the clockwise HE_{+11} mode and the anti-clockwise HE_{-11} mode [8]. The ferrite 2 disk provides an additional degree of freedom allowing impedance matching. It has influence on the in-phase TM_{01} mode without significantly impacting the rotational modes. In this purpose, the ferrite 2 disk is smaller in diameter than the ferrite 1 disk. The dimensioning of the planar ferrite resonator (ferrite 1) depends only on the in-phase TM_{01} mode when considering a demagnetized junction, hence the effective permittivity of the junction. In the proposed structure, the junction consists of regions {1} to {4} shown in Figure 5(b). Here, identical ferrite materials are considered for both disks. The diameter of the ferrite 1 is given by the following equation [9].

$$D_{f1} = \frac{1.84}{\pi\sqrt{\epsilon_{reff}}} \lambda_0, \quad (1)$$

where λ_0 is the wavelength in air at the central frequency and ϵ_{reff} is the effective relative permittivity of the junction. Considering the conservation of the series capacitances located between regions {1}, {2} and {3+4} and the parallel capacitance of regions {3} and {4}, the following relation is obtained:

$$\frac{H}{\epsilon_{reff}} = \frac{H_{f1}}{\epsilon_{rf}} + \frac{H_{f2}}{\epsilon_{req}} + H - (H_{f1} + H_{f2}), \quad (2)$$

with

$$D_{f1}^2 \epsilon_{req} = D_{f2}^2 \epsilon_{rf} + (D_{f1}^2 - D_{f2}^2), \quad (3)$$

where ϵ_{rf} and ϵ_{req} are respectively the relative permittivity of the ferrite material and equivalent permittivity of the region {3+4}, and H is the junction height.

According to the preceding relations, several solutions satisfy equation (1). To evaluate the possible solutions, the Matlab software is used to obtain the possible sets of solutions, varying D_{f1} by steps of 0.2 mm and H_{f1} and H_{f2} by steps of 0.1 mm, while complying with the following conditions: $D_{f1} > 2D_{f2}$ and $H > H_{f1} + H_{f2}$. Then the obtained sets of solutions are evaluated using CST electromagnetic (EM) software to select the optimal theoretical dimensions. After this initial pre-dimensioning step, an optimization phase is conducted using the EM software to center the frequency response within the desired operating band. Utilizing lithium ferrite, the results shown in Figure 3 achieve a return loss and isolation better than 25 dB across the entire 17.3 to 21.2 GHz frequency range, without employing any metallic ridges. This demonstrates that the capacitive effect provided by the ferrite 2 disk facilitates impedance matching between the junction and the AFSIW waveguide arms.

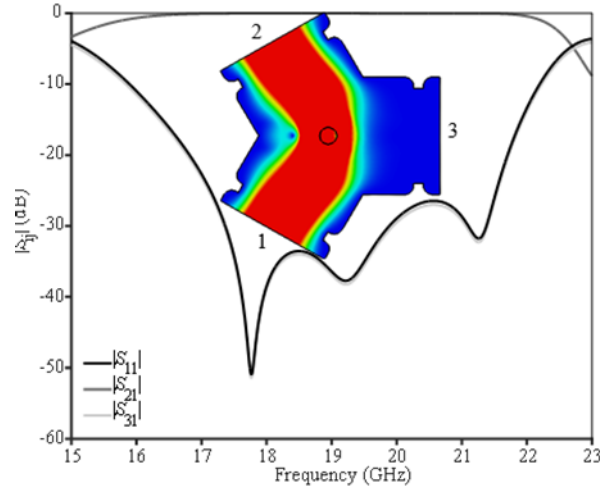


Figure 6. Simulated S-parameters of the magnetized junction for internal magnetic field of 10 Oe with the power flow magnitude distribution simulated at 19.5 GHz.

Following the design of the circulator, it was integrated with an AFSIW load as reported in [10]. The isolator was fabricated using multilayer technology and its performance was evaluated with a test fixture, depicted in the Figure 7(a), specifically designed for measuring AFSIW components [5]. An AFSIW TRL calibration kit was used to de-embed cables and interconnection effects. The reference planes are shown in Figure 7(a). Figure 7(b) compares the simulated and experimental small-signal results. A very good agreement between simulation and measurement is obtained. The proposed AFSIW isolator achieve a return loss, isolation and insertion loss better than 21 dB, 22 dB and 0.3 dB respectively.

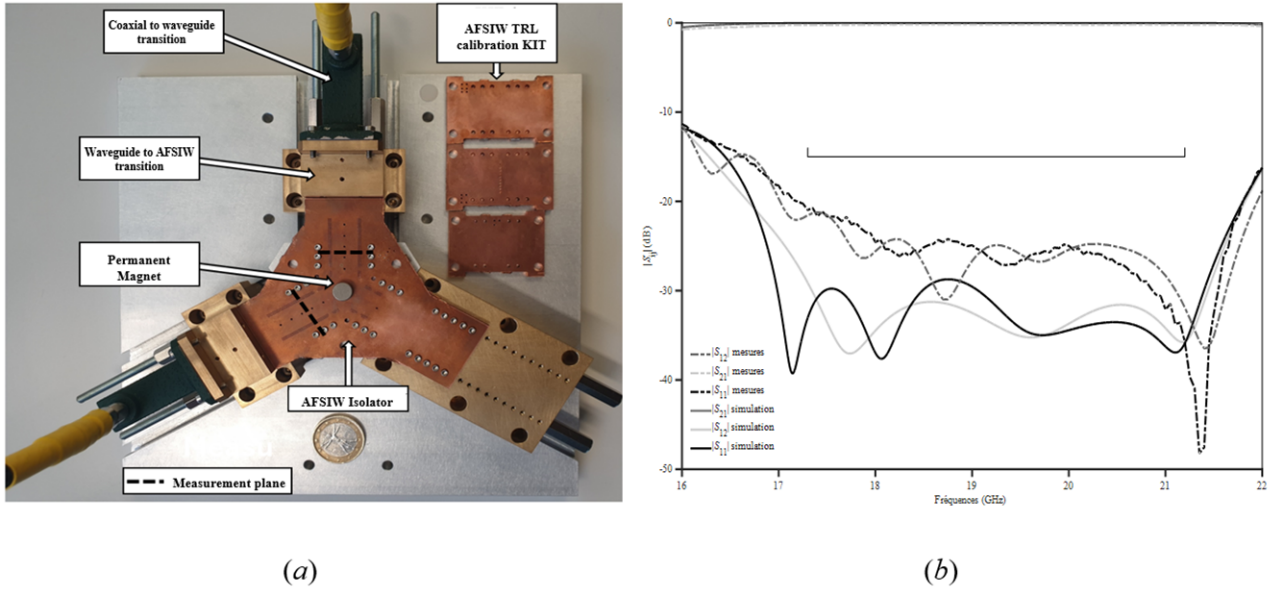


Figure 7. (a): AFSIW isolator measurement setup and (b): measurement vs simulated results.

Chanel Filter Design

After the realization and validation of the basic components, including the waveguide-to-AFSIW transition and a dual-junction circulator and isolator, the next step is to design the key elements of the duplexer, namely the channel filters. In this regard, the thesis [11] reported several implementations of bandpass filters that target the same frequency band as this thesis. Based on these works [11], the two channel filters are designed using rectangular AFSIW cavities coupled via inductive irises. To meet the rejection specifications, the proposed topology for the channel filters is a fourth-order filter consisting of four cavities and five coupling irises, as illustrated in Figure 8.

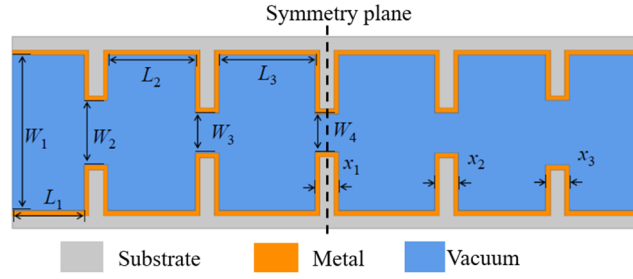


Figure 8. AFSIW channel filter.

The filters were dimensioned using the FEST 3D software. Table 1, along with Figure 9, illustrates the dimensions and frequency responses of each filter.

Table 1. AFSIW channel filter dimensions.

| Channel | Frequency (GHz) | W_1 (mm) | W_2 (mm) | W_3 (mm) | W_4 (mm) | L_1 (mm) | L_2 (mm) | L_3 (mm) | $x_{1,2,3}$ (mm) |
|---------|-----------------|------------|------------|------------|------------|------------|------------|------------|------------------|
| #1 | 18.87 | 12.96 | 6.18 | 3.89 | 3.75 | 5 | 8.14 | 9.09 | 1.51 |
| #2 | 20.50 | 12.96 | 5.37 | 3.31 | 3.07 | 5 | 7.24 | 7.97 | 2 |

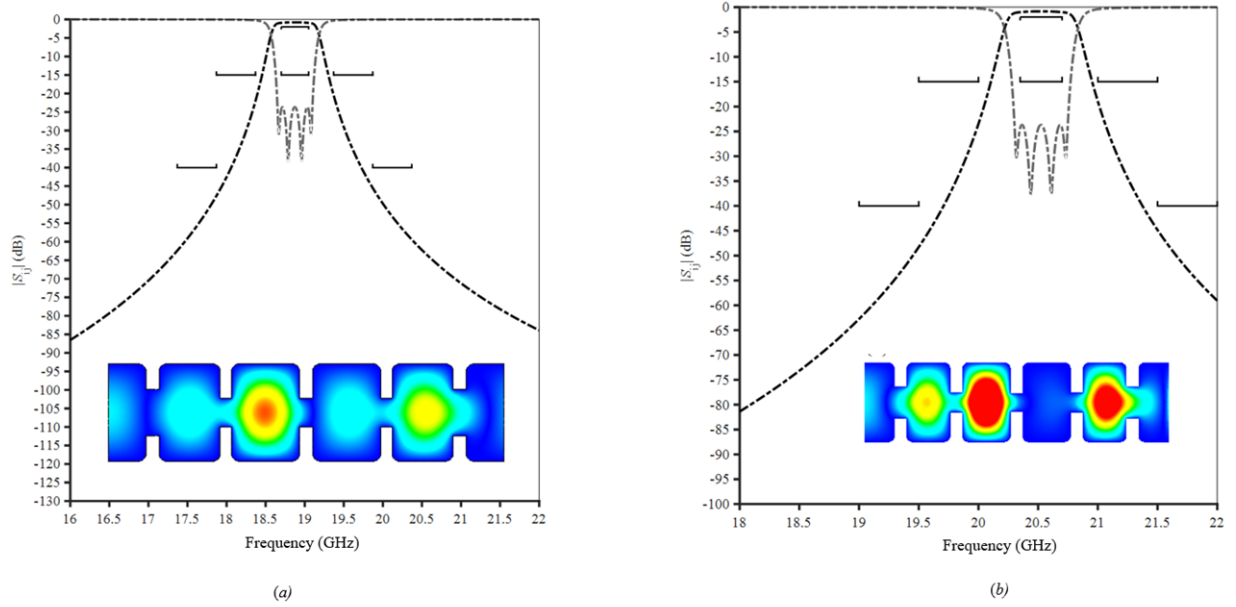


Figure 9. AFSIW channels filter S-parameters (a): channel #1 and (b): channel #2.

DUPLEXER DESIGN

Once the channel filters were designed, they were directly integrated with the basic components presented in the previous sections to achieve the duplexer function. The coupling of each channel is facilitated by a circulator. This configuration is particularly advantageous as it allows for independent operation of each filter, ensuring a simplified design without the need for a global EM optimization of the device. Figure 10 illustrates the proposed AFSIW duplexer.

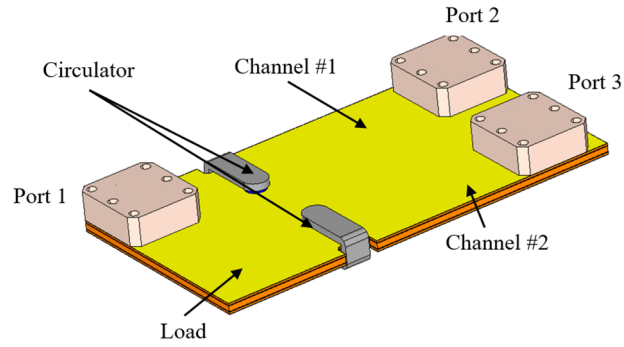


Figure 10. AFSIW duplexer.

For demonstration purposes, the AFSIW duplexer illustrated in Figure 11 was designed, fabricated, and measured to evaluate the electrical performance and validate the design model described in the previous section.

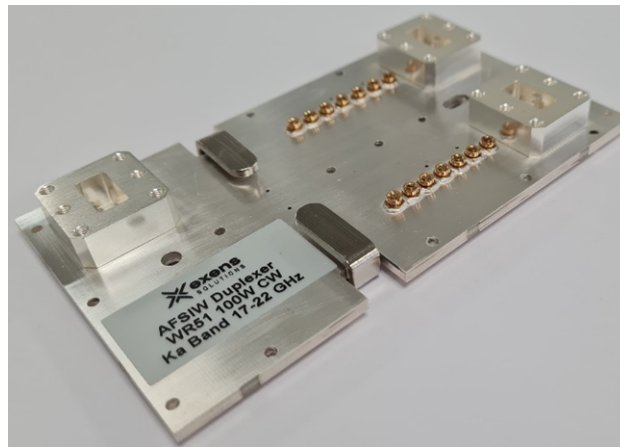


Figure 11. AFSIW duplexer prototype.

The duplexer was fabricated using three layers of RT/Duroid 6002 substrate. Substrate S2 has a thickness of $H_{s2} = 1.52\text{mm}$, identical to the thickness chosen in the previous section. Substrates S1 and S3 do not play any electromagnetic role; they are used in this design solely for mechanical support. However, they influence the distance between the magnets and ferrites, as well as the dissipation of power absorbed by the ferrites and converted into thermal heat via the Joule effect.

The ferrites, absorbers, and WR51 flanges were cut using a CNC machine to achieve the desired shape and dimensions. The ferrites and absorbers were then bonded using a low-thickness, low-EM-loss epoxy adhesive.

For the polarization of the double-junction circulators with saturated ferrite, two samarium magnets, and a remanent magnetic field of 0.92 T were used. The two magnets were each glued to the outer surfaces of substrates S1 and S3. Two mild steel yokes, as illustrated in Figure 10, were used to ensure the proper operation of the AFSIW duplexer and its magnetostatic sealing.

To compensate for the effects of manufacturing tolerances on the duplexer's performance, tuning screws were introduced in the waveguide-to-AFSIW transition, as well as in the cavities and irises of each channel filter. The measurements were carried out using a vector network analyzer, and a TRL WR51 calibration kit in waveguide technology to eliminate the effects of transitions and cables. The simulation and measurement results of the fabricated AFSIW duplexer prototype are illustrated in Figure 12 and 13. A good agreement between the simulation and experimental results was achieved.

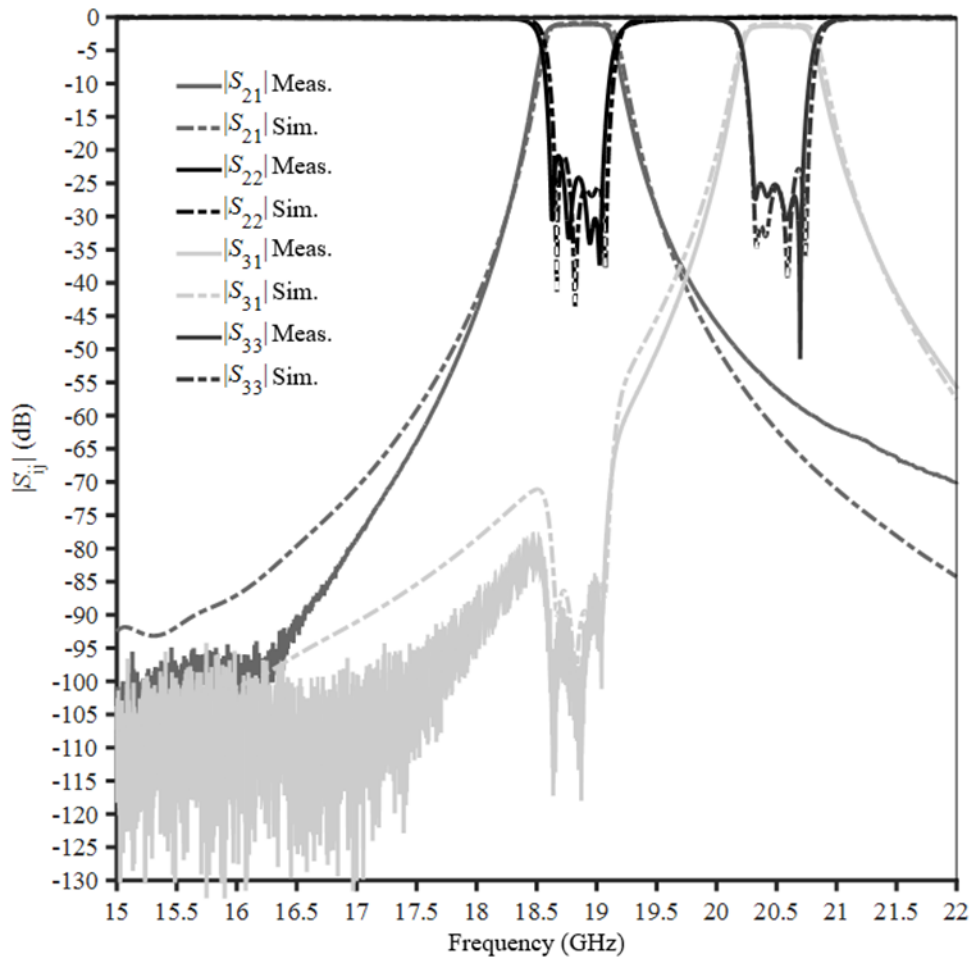


Figure 12. AFSIW Duplexer Simulation vs Measurement insertion and return loss.

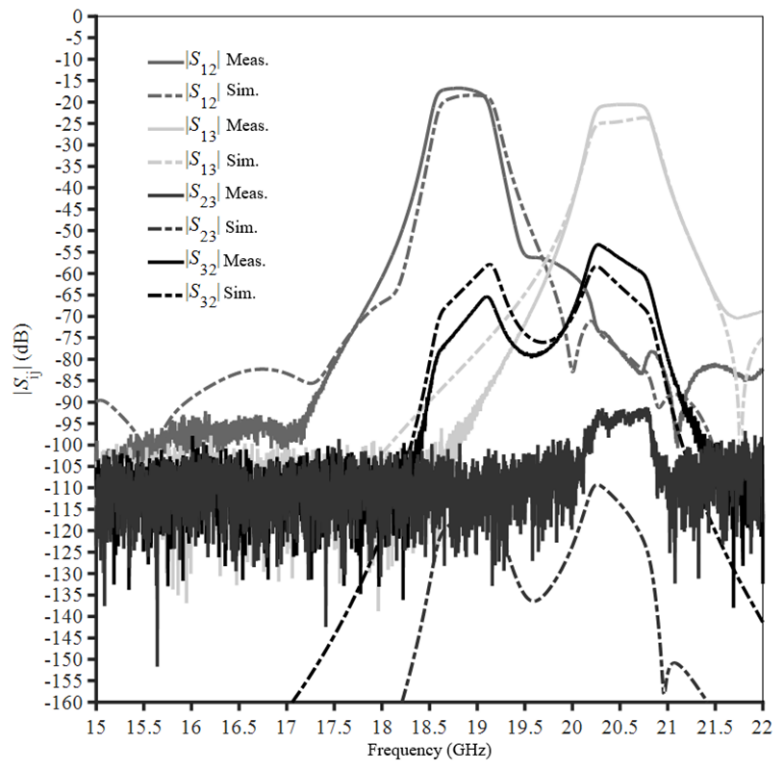


Figure 13. AFSIW Duplexer Simulation vs Measurement isolations.

To evaluate the duplexer performance under different environmental conditions, measurements were conducted at temperatures ranging from -20 °C to 85 °C. These measurements are illustrated in Figure 14, showing the transmission and matching of the duplexer channels at -20 °C, 23 °C, and 85 °C. The results demonstrate good thermal stability of -20 ppm for the AFSIW duplexer. Tables 2 and 3 summarize the measurement results of the duplexer across the temperature range from -20 °C to 85 °C. The measurement results confirm the proper functioning of the duplexer and its compliance with the required specifications in terms of matching, insertion loss, and isolation.

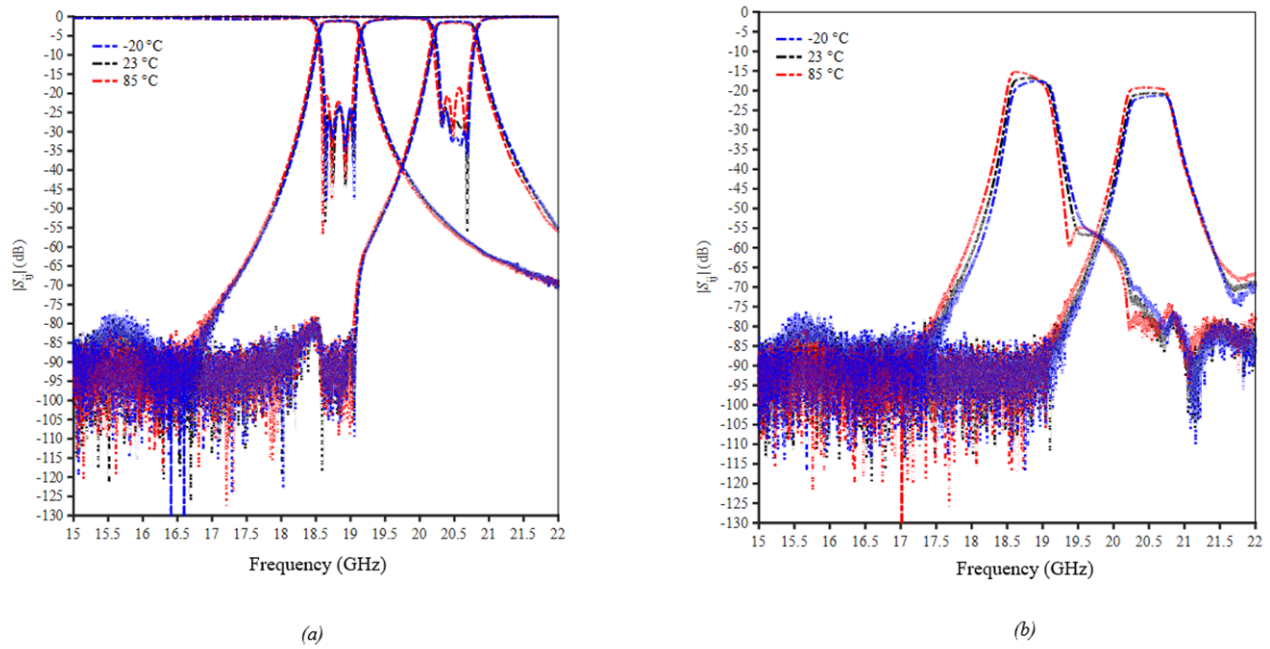


Figure 14. AFSIW Thermal test -20°C to 85°C, (a): insertion and return loss and (b): isolations.

Table 2. Measurements vs specification of channel #1 of the AFSIW duplexer across the temperature range from -20 °C to 85 °C.

| Frequency (GHz) | Parameter | | Specification | Measurement |
|-----------------|----------------|-----------------|---------------|-------------|
| 18.7-19.05 | Return loss | $ S_{11} $ (dB) | >15 | > 20 |
| | | $ S_{22} $ (dB) | | > 22 |
| | Insertion loss | $ S_{21} $ (dB) | < 2 | < 1.4 |
| | | Isolation | | > 19 |
| 17.37-17.87 | Rejection | $ S_{21} $ (dB) | > 40 | > 49 |
| 17.87-18.87 | | | > 20 | > 19 |
| 19.37-19.87 | | | > 20 | > 21 |
| 19.87-20.37 | | | >40 | > 42 |

Table 3. Measurements vs specification of channel #2 of the AFSIW duplexer across the temperature range from -20 °C to 85 °C.

| Frequency (GHz) | Parameter | | Specification | Measurement |
|-----------------|----------------|-----------------|---------------|-------------|
| 20.37-20.7 | Return loss | $ S_{11} $ (dB) | >15 | > 20 |
| | | $ S_{33} $ (dB) | | > 18 |
| | Insertion loss | $ S_{31} $ (dB) | < 2 | < 1.69 |
| | | Isolation | | > 19 |
| 19-19.5 | Rejection | $ S_{31} $ (dB) | > 40 | > 48 |
| 19.5-20 | | | > 20 | > 21 |
| 21-21.5 | | | > 20 | > 18 |
| 21.5-22 | | | >40 | > 41 |

CONCLUSION

This work presents the design of an AFSIW duplexer interconnected with waveguides operating in the Ka band for downlink applications, adhering to industrial specifications. The design is based on two channel filters coupled through a double junction comprising a circulator and an isolator.

To interconnect the duplexer, a transition from waveguide to AFSIW was studied. This design utilizes impedance transformers implemented through steps integrated within the waveguide and the multilayer PCB of the AFSIW line. The waveguide to AFSIW transition was successfully realized and measured, demonstrating low insertion losses (maximum 0.2 dB) and a wide bandwidth (25%).

The central element of the duplexer, consisting of a double junction (circulator and isolator), was designed by incorporating the broadband circulator and a load. The isolator was fabricated and measured under low signal conditions for demonstration purposes.

Following the validation of the elementary building blocks of the duplexer, fourth-order AFSIW channel filters were synthesized and designed independently to meet the required specifications in terms of rejection and impedance matching. These filters were then integrated into the overall assembly of building blocks. Once the duplexer design was finalized, it was fabricated, assembled, and measured under low signal conditions across a temperature range of -20 to 85 °C. The obtained results demonstrate that this new development extends the PCB capabilities and opens the door for the substrate integration of high-power microwave circuits and systems envisioned by the authors to be deployed by the industry, particularly for the new space applications.

REFERENCES

- [1] J. Uher, J. Bornemann, and U. Rosenberg, *Waveguide Components for Antenna Feed Systems—Theory and CAD*. Norwood, MA: Artech House, 1993.
- [2] R. J. Cameron, C. M. Kudsia, and R. R. Mansour, *Microwave Filters for Communication Systems*, Hoboken, NJ, USA: Wiley, 2007, ch. 14, pp. 501-530.
- [3] G. Matthaei, L. Young, and M.T. Jones, *Microwave Filters, Impedance Matching Networks and Coupling Structures*. Norwood, MA: Artech House, 1985.
- [4] T. Martin, F. Parment, A. Ghiotto, T. -P. Vuong, and K. Wu, "Air-Filled SIW interconnections for high performance millimeter-wave circuit and system prototyping and assembly," 2017 IEEE MTT-S International Conference on Numerical Electromagnetic and Multiphysics Modeling and Optimization for RF, Microwave, and Terahertz Applications (NEMO), 2017, pp. 302-304.
- [5] I. Marah, A. Ghiotto, A. Verger and J. -M. Pham, "A Test Fixture for the Measurement of 3-port Y-junction AFSIW Circuits," 2021 IEEE MTT-S International Microwave Workshop Series on Advanced Materials and Processes for RF and THz Applications (IMWS-AMP), Chongqing, China, 2021, pp. 305-307,
- [6] I. Marah, A. Ghiotto, J. -M. Pham, A. Verger and É. Laroche, "Reduced-height Waveguide Y-Junction Circulator Based on Two Asymmetrical Gyromagnetic Posts," 2021 IEEE MTT-S International Microwave Symposium (IMS), Atlanta, GA, USA, 2021, pp. 657-660.
- [7] French Patent FR2101524A "Non-reciprocal microwave component," Inventors: I. Marah, A. Verger, A. Ghiotto and J. -M. Pham, Feb 2021.
- [8] B. Owen, "The identification of modal resonances in ferrite loaded waveguide Y-junctions and their adjustment for circulation," in *The Bell System Technical Journal*, vol. 51, no. 3, pp. 595-627, Mar. 1972.
- [9] E. J. Denlinger, "Design of partial height ferrite waveguide circulators (Short Papers)," in *IEEE Transactions on Microwave Theory and Techniques*, vol. 22, no. 8, pp. 810-813, Aug. 1974.
- [10] I. Marah, A. Ghiotto, J. -M. Pham, T. Martin and A. Boisse, "AFSIW Termination with Full- and Partial-Height Absorbing Material Loading," 2019 49th European Microwave Conference (EuMC), Paris, France, 2019, pp. 686-689.
- [11] T. Martin, "Air-filled substrate integrated waveguide (AFSIW) filters and multiplexers for space application," Thèse de doctorat en électronique, sous la direction de Anthony Ghiotto, Bordeaux, Université de Bordeaux, 2020.